17th Brazilian Congress of Thermal Sciences and Engineering
November 25th-28th, 2018, Águas de Lindóia, SP, Brazil

ENCIT-2018-0669
A NUMERICAL METHOD FOR HIGH RESOLUTION SIMULATION OF SOLID-LIQUID FLOW USING DEM

Roderick Gustavo Pivovarski
Joviano Janjar Casarin
Alan Lugarini de Souza
Admilson Teixeira Franco
Universidade Tecnológica Federal do Paraná, Rua Deputado Heitor Alencar Furtado, 5000, CEP 81280-340
roderick@alunos.utfpr.edu.br
jovianocasarin@utfpr.edu.br
alansouza@utfpr.edu.br
admilson@utfpr.edu.br

Abstract. *The motion of solid particles dispersed in viscous fluids is of great interest in several industries. In the particular case of oil industry, cuttings from oil wells are carried away by drilling fluids, and the acting forces between solid and liquid phases dictate the two-phase flow regime. This paper focuses on the numerical calculation of the forces acting on a single spherical particle immersed in different fluids, such as air, water and silicone oil, using both one and two-way coupling between the particle and the continuous phase, in a Eulerian-Lagrangian framework. Firstly, using one-way coupling between fluid and particle, numerical methods are compared in order to properly model the forces acting on the particle: drag, Magnus lift, Saffman's lift, Basset's (history), pressure gradient, drag torque and virtual mass. Forces originated from collisions between the particle and a surrounding wall are accounted for by the Discrete Element Method (DEM) with a simple linear-spring model. Results show that the history term is indispensable when it comes to calculating the motion of a bouncing particle immersed in a viscous liquid, and DEM correctly models the impact of the bead. When two-way coupling is used to account for the influence of the solid phase on the surrounding fluid, other factors become important and the grid size may be constrained by traditional numerical methods. A promising alternative approach that re-distributes the momentum source term in the neighboring cells is implemented and analyzed. Validation tests show that this alternative manages to better represent real physical phenomena.*

Keywords: Discrete element method, two-way coupling, momentum distribution, source smoothing method.

INTRODUCTION

At the current industrial scenario, the number and variety of processes in which particulate flows are present is considerable. Pharmaceutical, food, mineral, chemical and oil industries constitute an example. Hence, the overall performance and design improvements on these processes rely upon the knowledge of complex systems in which particles interact with a fluid media and with another solid bodies (KHARAZ et al. 2001).

In practice, the number of solids present within the system may vary in a considerable range; from some hundreds until more than a billion per cubic meter (KRUGGEL-EMDEN et al., 2007). Thus, the forces originated from collisions between solid entities are as import as the forces that come from hydrodynamic interactions.

Many works have dealt with solid-liquid flows, since this phenomenon is present at several cases of interest in the industry. Some examples regarding the oil industry were carried out at the Center of Research in Rheology and non-Newtonian Fluids (CERNN). De Lai (2013) and Barbosa (2015) used a solid-liquid flow in order to control the invasion, a process that consists of losses of drilling mud to the reservoir. Poletto (2017) studied the formation of a mud cake in the walls of an oil well, process that consists of the deposition of particles throughout a porous media. These studies show the importance of studying flows consisting on the interaction of solid and liquid phases.

Then, in order to numerically study the behavior of a single particle interacting with a fluid and solid bodies, two-way coupling simulations have been made aiming to reproduce experimental and numerical results available in the literature. Despite the fact that this coupling is better justified when a high volume fraction of the dispersed phase is present, its ability to correctly monitor the behavior of the particle indicates that the coupling between the phases is correctly accounted for.

In this paper the importance of the correct distribution of momentum between the two phases in a solid-liquid flow is investigated, which has a great appeal, since this is a paramount condition to monitor adequately the physics of the phenomenon. In order to fulfill this, validations cases are ran to show that it can be made, even using a refined grid, which consisted in a constrain on previous simulations.

MATHEMATICAL FORMULATION

The mathematical approach to the problem is elaborated in the following way: the modified continuity and Navier-Stokes equations are solved in an Eulerian framework to the fluid phase, which means that the volumetric average behavior of the fluid is considered. For the solid dispersed phase, a Lagrangian approach is used, in which each particle is individually treated using Newton's law for the motion. The two-way coupling consists in a source term in the modified Navier-Stokes equation of the fluid phase and the use of a parameter that monitor the cell fraction that is occupied by fluid. Equation (1) shows the modified continuity equation as shown in(PEKER; HELVACI, 2011):

$$\frac{\partial(\varepsilon_f \rho_f)}{\partial t} + \nabla \bullet (\varepsilon_f \rho_f \mathbf{u}_f) = 0 \tag{1}$$

Where ε_f is the volume fraction of the fluid phase, ρ_f its density and $\mathbf{u}_f$ the velocity vector of the fluid. The modified Navier-Stokes equation for the fluid is:

$$\frac{\partial(\varepsilon_f \rho_f \mathbf{u}_f)}{\partial t} + \nabla \bullet (\varepsilon_f \rho_f \mathbf{u}_f \mathbf{u}_f) = -\varepsilon_f \nabla p + \varepsilon_f \nabla \bullet \tau + \varepsilon_f \rho_f \mathbf{g} - \mathbf{S}_f \tag{2}$$

Where p is the pressure field of the fluid phase, τ is the viscous stress tensor, $\mathbf{g}$ the gravity field and $\mathbf{S}_f$ is the so-called source term that account for the momentum exchange between the phases. The source term is calculated summating all the forces acting on the particles inside a particular cell and dividing it by the volume of this cell, so it becomes (AKHSHIK; BEHZAD; RAJABI, 2015):

$$\mathbf{S}_f = \frac{\left(\sum_{i=1}^{n} \mathbf{F}_i\right)}{V_{cell}} \tag{3}$$

In Equation (3), the numerator represents the sum of the forces acting on all the particles within a particular control volume (cell), and V_{cell} is the volume of this cell. Calculating the source term correctly is a fundamental aspect of any solid-liquid simulation, since this is the term that accounts the energetic interaction between the phases. For the particle, the Newton's law for motion is given by Equation (4):

$$m_p \frac{d\mathbf{u}_p}{dt} = \mathbf{F}_{gb} + \mathbf{F}_D + \mathbf{F}_{pg} + \mathbf{F}_{vm} + \mathbf{F}_l + \mathbf{F}_{history} + (\mathbf{F}_{\mathrm{DEM}}) \tag{4}$$

where m_p and $\mathbf{u}_p$ are the particle's mass and velocity vector, respectively. The forces on the right hand side (RHS) of Equation (4) are discussed on APPENDIX A. The Discrete Element Method, used to calculate the forces originated from collisions, and denoted by the term $\mathbf{F}_{\mathrm{DEM}}$, is better explained in the APPENDIX B.

The Newton's law for conservation of the angular momentum acting on the particle is given by Equation (5):

$$I_p \frac{d\boldsymbol{\omega}_p}{dt} = \mathbf{T}_D + \mathbf{T}_{DEM} \tag{5}$$

where I_p is the moment of inertia of the particle, $\boldsymbol{\omega}_p$ its angular velocity, $\mathbf{T}_D$ is the drag torque created by the interaction with the fluid and $\mathbf{T}_{\mathrm{DEM}}$ is the torque created by collisions with other solid entities. Following the procedure that was done to the forces calculated with DEM's aid, the torque also may be split in two components. Doing so, and using the notation of AKHSHIK, BEHZAD, RAJABI (2015), Equation (5) becomes:

$$I_p \frac{d\boldsymbol{\omega}_p}{dt} = \mathbf{T}_D + \left(\mathbf{T}^p{}_{t,q} + \mathbf{T}^p{}_{r,q}\right) \tag{6}$$

the first term on the RHS of Equation (6) represents the torque experimented by the particle due to its interaction with the surrounding fluid, and is therefore called drag torque. This torque tends to slow down the particle's rotation movement (LUKERCHENKO et al., 2012). Its expression is given by Equation (7):

$$\mathbf{T}_D = -C_\omega \frac{\rho_p}{64} \boldsymbol{\omega}_p \left|\boldsymbol{\omega}_p\right| D_p^{\,5} \tag{7}$$

where C_ω is the dimensionless drag torque coefficient, and the minus sign indicates that the drag torque acts on the opposite direction of the particle's angular velocity vector. The last two terms of Equation (6) are calculated using the DEM, and, for this reason, are discussed on the Appendix B.

The term that in fact characterizes the coupling between the phases is the source term, given in Equation (3) and placed in Equation lap. One particular feature of simulations with a solid phase is that the cell volume must be greater than the particles' volume. This restriction comes from the fact that, in Equation (3), the momentum of the fluid is calculated considering its volume fraction in a cell. When this value approaches zero, CFD softwares start to have problems calculating the moment for the fluid phase. On the other hand, a course grid might be a wrong choice when it comes to capture the details of the fluid phase flow, since there will always be a velocity gradient near the walls due to the no-slip condition.

METHODOLOGY

This constrain can be overcame with the aid of the source smoothing method, a commercial tool provided by *STAR-CCM+*®. The main idea is to create a cluster using original cells, originating bigger cells to which the momentum of the particles is transferred, *i.e.*, the denominator in Equation (3) gets a bigger value, quelling the possibility of instabilities of the solver. After that, the software divides the total amount of moment between the cells of the original refined grid according to the volume of the cell that is occupied by the particle. It is important to mention that, for the momentum exchanged between the fluid cells, the original grid is used, not affecting the fluid flow at any moment. This tool have a paramount importance in simulations of particulate flows in confined spaces such as pipes, in which velocity gradients must be accounted for. An important parameter of the source smoothing method is the 'Scale', responsible to define the size of the cell originated by the clustering of the original smaller cells. Scale equals two means that the clustered cell will have edges whose length correspond to the double of the edges of the biggest cell in the original domain. Using Scale equals five means that the characteristic length will be 5 times larger, and so on. Figure 1 illustrates which cells receive momentum from the solid phase with and without the use of the source smoothing method.

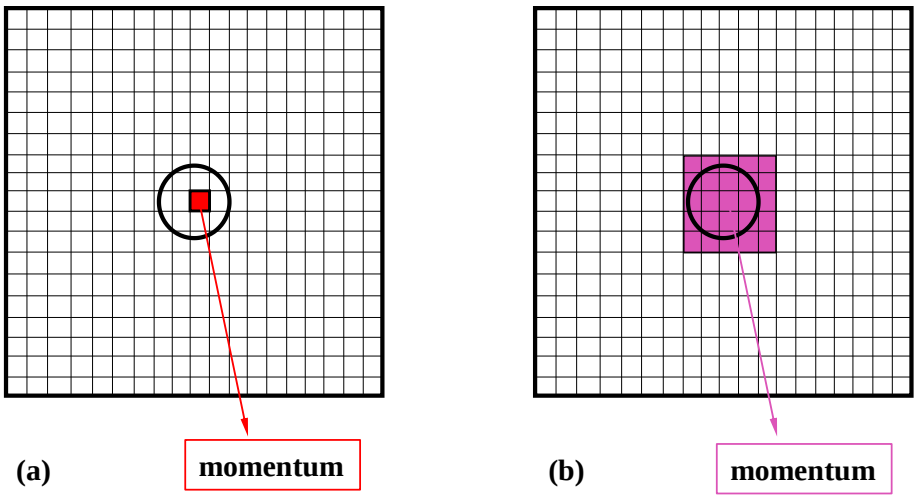

Figure 1 - Illustration of the cells that receive momentum from the solid phase. (a) Scale = 1. (b) Scale = 5.

An important aspect of every numerical simulation is the boundary conditions used. Since all the cases run for the elaboration of this paper consisted of a single particle settling in a fluid, all the boundary conditions were the same, *i.e.*, a fluid domain surrounded by walls with an opening to the environment at the top of the vessel, represented by a pressure outlet.

The following section discusses the results obtained.

RESULTS

To validate the simulations with the two-way coupling between the phases, comparisons were made with experimental data available in the literature, regarding the sedimentation of particles in several fluids, such as water and silicone oil. Figure 2 shows the results for the terminal velocity of a 1 mm diameter glass sphere (density = 2560 [kg/m³])

settling in water (density = 997 [kg/m³] and dynamic viscosity = 8.9 x 10^{-4} [Pa.s]), compared with the experiments carried out by Mordant & Pinton (2000).

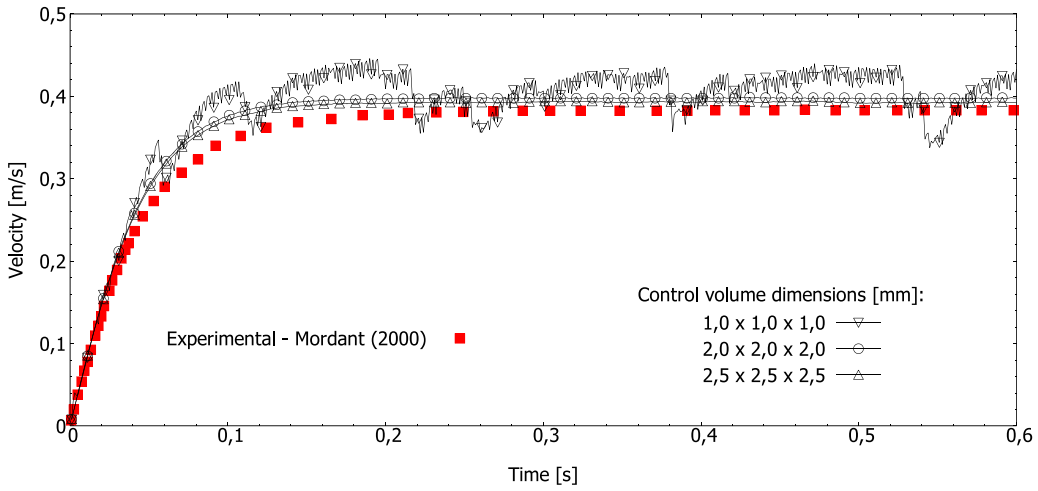

Figure 2 - Results for the terminal velocity of a glass sphere of diameter 1 [mm] settling in water.

Figure 2 shows the importance of using a control volume bigger than the particle's diameter. For a control volume whose edges are of the same size of the particle, the velocity shows a completely irregular pattern. For bigger cells, the simulations give a very good result for both the transient and permanent velocity of the sphere. It is important to mention that, the cubic 2.5 [mm]-edged cell grid gives better results compared to the one of 1 [mm] edges. This fact illustrates that, in order to account correctly the momentum exchange between the phases, the cell must be bigger than the particle.

Figure 3 shows the trajectory obtained by Lukerchenko et al. (2012).for a 3.65 cm sphere of density 971 [kg/m³] with initial angular velocity 178.5 [rad/s] and initial translational velocity of 0.412 [m/s] moving throughout water.

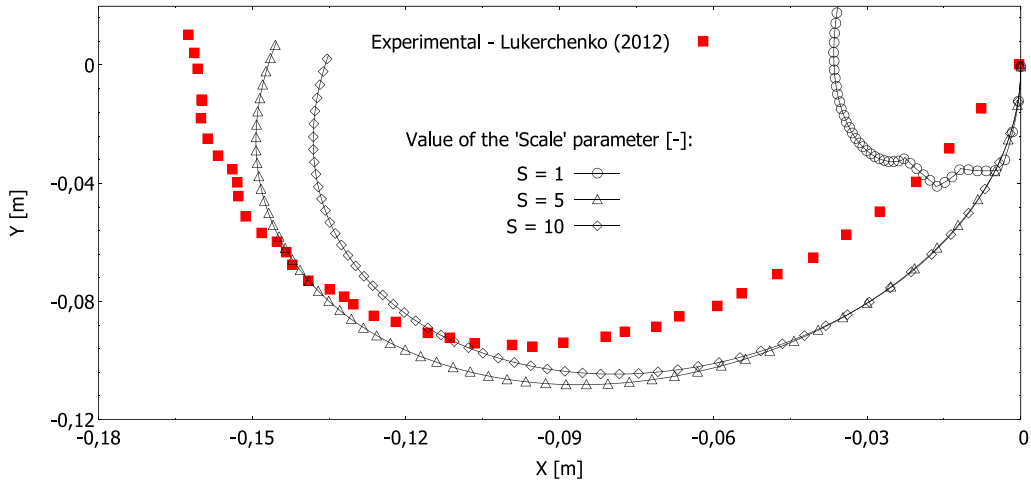

Figure 3 - Results for the trajectory of a 3.65 cm diameter sphere with initial angular velocity of 178.5 [rad/s] and initial translational velocity of 0.412 [m/s] moving through water.

In this simulation, the size of the cells was fixed: each cell consisted of a cube in which the edges had the same length of the particle's diameter, *i.e.*, 3.65 [cm]. It is possible to see the big contrast when the simulation is done with the scale parameter equals one and when its value is bigger than one, *e.g.* five and ten. The results of the simulations carried out with bigger values for the Scale parameter resemble much better the experimental results of Lukerchenko et al. (2012). However, it is evident that, for this case, an intermediate value of five to the scale parameter gives a better fit to the curve compared to that obtained when the value used for the Scale was 10, showing that the value of the parameter must be carefully chosen; it cannot be too small neither too big.

A good rule of thumb for the choice of the value of the Scale could be the following: the result of the division between the volume of the biggest cell in the domain and the particle's volume is a good guess for the value of the Scale parameter. A drawback for this rule is that it might be easy to carry out when the grid is composed by regular cells; however, when the grid is made of irregular cells, it can be difficult.

A final evidence of the importance of the Scale parameter is shown in Figure 4. It shows the transversal displacement of the particle normalized by its diameter on the x-axis, while the y-axis shows the particle's coordinate in the vertical direction. When the scale parameter used is equal one, the particle exhibits a transversal translation of that reaches almost 40 percent of its diameter. On the other hand, when the value of the Scale parameter is two and five, the maximum displacements correspond to 18 and 3.8 percent respectively, depicting the instability generated by an erroneous momentum transfer between the solid and liquid phase. The case consists in a spherical particle settling in silicon oil (ρ_f = 935 [kg/m³] and μ_f = 0.01 [Pa.s]).

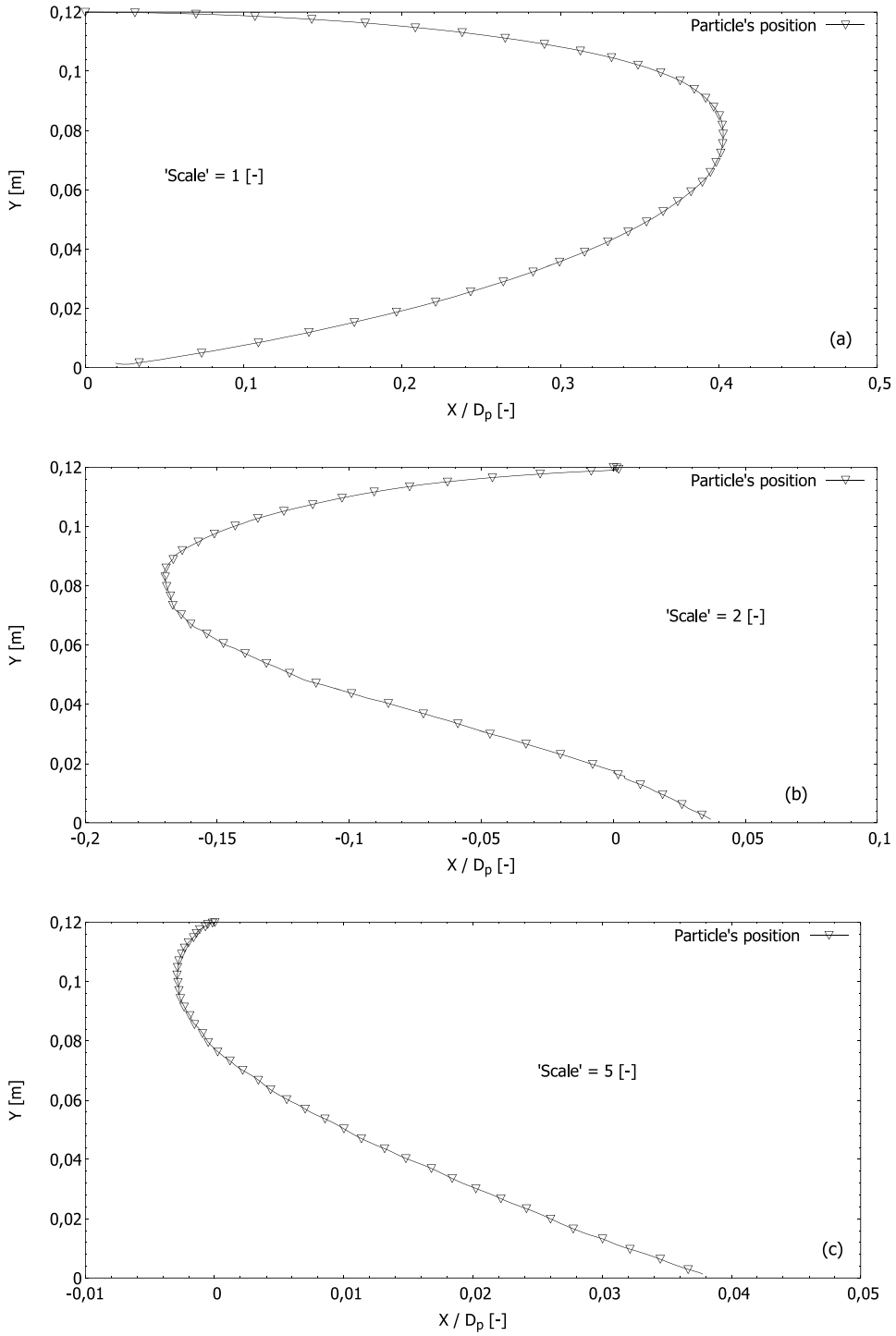

Figure 4 - Comparison of the transversal movement of the particles obtained when using different values for the Scale parameter. (a) Scale = 1. (b) Scale = 2. (c) Scale = 5.

CONCLUSIONS

We conclude from the results of this paper that the simulations using the Scale parameter were capable of representing very well results obtained experimentally. However, it happened only when the cell's volume was bigger than the particle's volume contained within it, so the momentum exchange could be done with accuracy. Therefore, there is a constrain on the grid size. It turns out that this constrain may limits the capability of reproducing velocity gradients in confined spaces, such as wellbores and pipelines. The source smoothing method is a promising numerical technique that might be used to overcome the problem mentioned, that is, represent solid-liquid and liquid-liquid momentum transfer within the same grid and, therefore, represent the real physical phenomena occurring. Additionally, one practical rule was proposed to estimate the value of the Scale parameter.

ACKNOWLEDGEMENTS

The authors of this paper would like to thank Petrobras and UTFPR/DAMEC for the support given.

REFERENCES

AKHSHIK, S.; BEHZAD, M.; RAJABI, M. CFD-DEM approach to investigate the effect of drill pipe rotation on cuttings transport behavior. Journal of Petroleum Science and Engineering, v. 127, p. 229–244, 2015.

BARBOSA, M. V. Análise paramétrica de escoamento particulado aplicado ao preenchimento de fraturas. 2015.

CUNDALL, P. A.; STRACK, O. D. L. A discrete numerical model for granular assemblies. Géotechnique, v. 29, n. 1, p. 47–65, 1979.

DE LAI, F. C. Simulação numérica do escoamento particulado para o preenchimento de canal fraturado. 2013.

DI RENZO, A.; DI MAIO, F. P. Comparison of contact-force models for the simulation of collisions in DEM-based granular flow codes. Chemical Engineering Science, v. 59, n. 3, p. 525–541, fev. 2004.

GONDRET, P.; LANCE, M.; PETIT, L. Bouncing motion of spherical particles in fluids. Physics of Fluids, v. 14, n. 2, p. 643–652, fev. 2002.

KHARAZ, A. H.; GORHAM, D. A.; SALMAN, A. D. An experimental study of the elastic rebound of spheres. Powder Technology, v. 120, n. 3, p. 281–291, 2001.

KRUGGEL-EMDEN, H. et al. Review and extension of normal force models for the Discrete Element Method. Powder Technology, v. 171, n. 3, p. 157–173, 2007.

KUANG, S. B.; YU, A B.; ZOU, Z. S. Computational Study of Flow Regimes in Vertical Pneumatic Conveying. p. 6846–6858, 2009.

LAWRENCE, C. J.; MEI, R. Long-time behavior of the drag on a body in impulisve motion. J. Fluid Mech., v. 283, p. 307–327, 1995.

LOTH, E. Particles, Drops and Bubbles: Fluid Dynamics and Numerical Methods. p. 1–345, 2010.

LUKERCHENKO, N. et al. Drag force, drag torque, and magnus force coefficients of rotating spherical particle moving in fluid. Particulate Science and Technology, v. 30, n. 1, p. 55–67, 2012.

MORDANT, N.; PINTON, J. F. Velocity Measurement of a Settling Sphere. European Physics Journal, p. 343–352, 2000.

PEKER, S. M.; HELVACI, S. S. Solid-Liquid Two Phase Flow. [s.l: s.n.].

POLETTO, V. G. MODELAGEM E SIMULAÇÃO NUMÉRICA DA DEPOSIÇÃO DE PARTÍCULAS EM MEIO POROSO: UM ESTUDO DA FORMAÇÃO DE REBOCO DURANTE A PERFURAÇÃO DE POÇOS DE PETRÓLEOCuritiba, 2017.

STONE, H. A. Philip Saffman and viscous flow theory. Journal of Fluid Mechanics, v. 409, p. 165–183, 2000.

APPENDIX A - FORCES ACTING ON A PARTICLE

In order to have a better understanding of the motion of a particle within a fluid environment, it is important to discuss each one of the forces on the RHS of Equation (4). That equation is rewritten here for commodity:

$$m_p \frac{d\mathbf{u}_p}{dt} = \mathbf{F}_{gb} + \mathbf{F}_D + \mathbf{F}_{pg} + \mathbf{F}_{vm} + \mathbf{F}_l + \mathbf{F}_{history} + (\mathbf{F}_{\mathrm{DEM}}) \tag{A.1}$$

$\mathbf{F}_{gb}$ is the force due to gravity and buoyancy, and is given by Equation (A.2) (LOTH, 2010):

$$\mathbf{F}_{gb} = m_p \left(\frac{\rho_p - \rho_f}{\rho_p} \right) \mathbf{g} \tag{A.2}$$

where $\mathbf{g}$ is the gravity field, ρ_p is the particle's density and ρ_f is the fluid's density. $\mathbf{F}_D$ is the drag force acting on the particle, and its expression is given by Equation (A.3) (PEKER; HELVACI, 2011)::

$$\mathbf{F}_D = -3\pi\mu_f D_p \mathbf{u}_p \tag{A.3}$$

where μ_f is the dynamic viscosity of the fluid phase and, D_p is the particle's diameter, and the minus sign indicates that the force acts on the direction opposite to that of the velocity vector of the fluid. Other force that acts on the particle is the pressure gradient force, given by the term $\mathbf{F}_{pg}$ in Equation (A.1). Its expression is given by (PEKER; HELVACI, 2011):

$$\mathbf{F}_{pg} = m_p \frac{\rho_f}{\rho_p} \left(\mathbf{u}_f \nabla \bullet \mathbf{u}_f \right) \tag{A.4}$$

where $\mathbf{u}_f$ is the velocity vector of the fluid phase, and ∇ is the nabla operator, given by Equation (A.5):

$$\nabla = \left(\frac{\partial}{\partial x}\hat{\mathbf{e}}_\mathbf{i} + \frac{\partial}{\partial y}\hat{\mathbf{e}}_\mathbf{j} + \frac{\partial}{\partial z}\hat{\mathbf{e}}_\mathbf{k} \right) \tag{A.5}$$

Continuing with the terms on the RHS of Equation (A.1), $\mathbf{F}_{vm}$ is the virtual mass force, and accounts for the mass of fluid that is accelerated by the particle, as if it was an extra mass added to this particle (PEKER; HELVACI, 2011). Its expression is given by Equation (A.6):

$$\mathbf{F}_{vm} = -C_{vm} m_p \frac{\rho_f}{\rho_p} \left\{ \frac{D\left(\mathbf{u}_p - \mathbf{u}_f\right)}{Dt} \right\} \tag{A.6}$$

where C_{vm} is the nondimensional virtual mass force coefficient, which is 0.5 for a spherical particle (GONDRET; LANCE; PETIT, 2002). The minus sign indicates that the force is opposite to the term inside the brackets on Equation (A.6). The term $\mathbf{F}_l$ refers to the lift forces, and may be split into two terms: The Magnus' lift force and the Saffman's lift force. Doing so, one obtains:

$$\mathbf{F}_l = \mathbf{F}_{lm} + \mathbf{F}_{ls} \tag{A.7}$$

The Magnus' lift force appears when a particle has both translational and rotational motion around its center of mass (PEKER; HELVACI, 2011). It is also known by Magnus' effect, and its expression is given by the following equation:

$$\mathbf{F}_{lm} = m_p \frac{\rho_f}{\rho_p} \left[C_M \bullet \boldsymbol{\omega}_p \times \left(\mathbf{u}_f - \mathbf{u}_p \right) \right] \tag{A.8}$$

where C_M is the nondimensional Magnus's force coefficient and $\boldsymbol{\omega}_p$ is the particle's angular velocity vector. The Saffman's lift force appears when the particle is confined within a closed device, such as a pipe. The no slip condition in the wall induces a velocity gradient on its surroundings, where particles may be translating. The combination of these effects generates the Saffman's lift force (STONE, 2000). Its expression is given Equation (A.9).

$$\mathbf{F}_{ls} = m_p \frac{\rho_f}{\rho_p}\left[C_{ls} \bullet \boldsymbol{\omega}_f \times \left(\mathbf{u}_f - \mathbf{u}_p \right) \right] \tag{A.9}$$

where C_{ls} is the nondimensional Saffman's lift force coefficient and $\boldsymbol{\omega}_f$ is the velocity vector of the fluid phase. Continuing with the forces present in Equation (A.1), $\mathbf{F}_{history}$ is the Basset's history term, a force that accounts for the cumulative effect of the transient wake of the particle (MORDANT; PINTON, 2000), and can be calculated using the expression developed by (LAWRENCE; MEI, 1995):

$$\mathbf{F}_{history} = -3\pi\mu_f \left(\mathbf{u}_p - \mathbf{u}_f \right) \phi_h(t) \tag{A.10}$$

where the minus signal denotes that the force acts in the opposite direction regarding the slip velocity between the particle and the fluid, and the term $\phi_h(t)$ takes into consideration the time-dependent behavior of the Basset's history force. $\phi_h(t)$ is given by the equation below:

$$\phi_h(t) = \frac{1.5\left(\phi_r + \mathrm{Re}_r\, \phi_r'\right)t}{(1+e)\phi_i} \tag{A.11}$$

In which e is the coefficient of restitution, and:

$$\phi = 1 + 0.15\,\mathrm{Re}^{0,687} \tag{A.12}$$

where Re is the particle's Reynolds number, given by $\mathrm{Re} = (\rho_f\, |\mathbf{u}_p|\, D_p)/2\, \mu_f$. The subscripts r and i are used to indicate that the ϕ parameter is evaluated at the incidence and after the rebound (before and after a collision). Mathematically:

$$\phi_r = -e\phi_i \tag{A.13}$$

Lastly, ϕ' is the derivative of Equation (A.12) in relation to the particle's Reynolds number. Then:

$$\phi' = 0.10305\,\mathrm{Re}^{-0,313} \tag{A.14}$$

Finally, the last term on the RHS of Equation (A.1), $\mathbf{F}_{\mathrm{DEM}}$, represents forces originated from collisions between particles (or between particles and walls) and is calculated using the Discrete Element Method. The APPENDIX B shows an overview into DEM, paramount to take interactions between particles into account on the simulations.

APPENDIX B - THE DISCRETE ELEMENT METHOD

The Discrete Element Method (DEM) was first introduced in the work of Cundall and Strack (1979), and is based in two main features. Firstly, when particles collide, they are allowed to overlap, originating forces and torques in normal and tangential directions. Secondly, the resultant forces and torques may be represented by discrete entities, such as springs and dashpots, who account, respectively, for repulsive forces and energy dissipation. Figures B.1 to B.3 highlight the main characteristics of the DEM, following the notation of the work carried out by Akhshik, Behzad and Rajabi (2015).

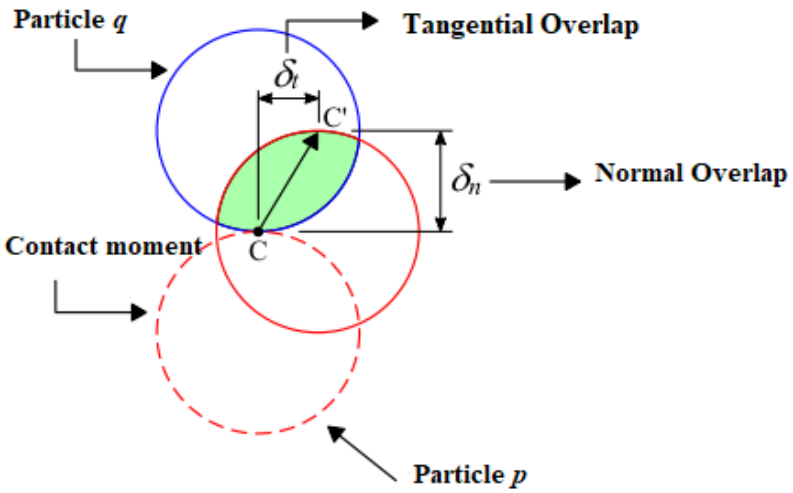

Figure B.1 - Overlaps used by the DEM to calculate the interaction between two spherical particles

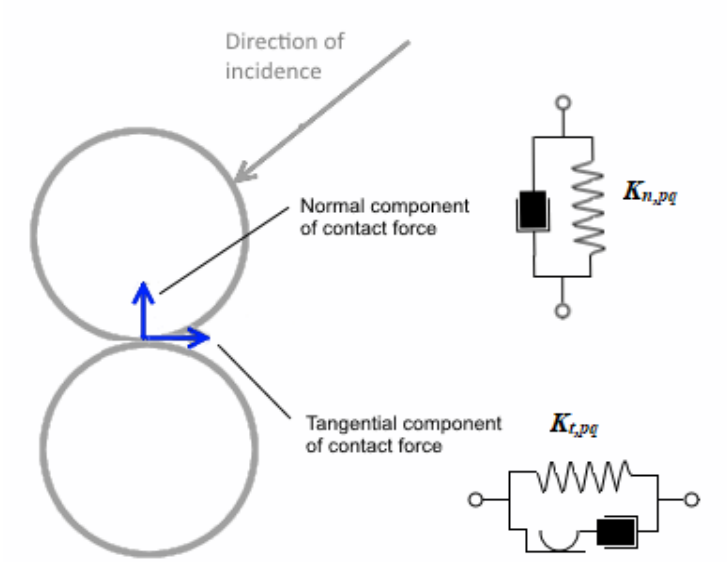

Figure B.2 - Discrete elements used to depict interaction between two particles using the DEM.

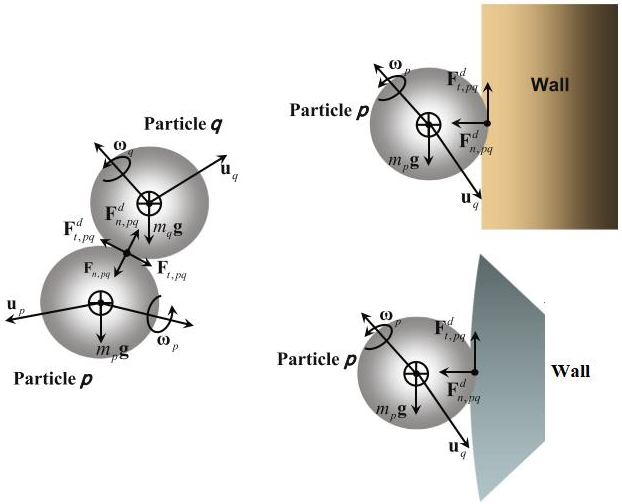

Figure B.3 - Forces originated from collisions in the Discrete Element Method. Source: Akhshik, Behzad and Rajabi (2015).

The forces generated by the DEM in a particle p may be written with the notation used in the work of Akhshik, Behzad and Rajabi (2015):

$$\mathbf{F}_{DEM,p} = \mathbf{F}_{n,pq} + \mathbf{F}_{t,pq} + \mathbf{F}^{d}{}_{n,pq} + \mathbf{F}^{d}{}_{t,pq} \tag{B.1}$$

Each one of the forces on the right term side of Equation (B.1) are now explained. According to Di Renzo and Di Maio (2004), the modulus of the normal force between the particles is given by:

$$\left|\mathbf{F}_{n,pq}\right| = -K_{n,pq}\delta_{n,pq} \tag{B.2}$$

where δ_n is the overlap and K_n is the elastic constant of the particles, both in the normal direction. The elastic constant depend upon physical and geometrical properties of the particles colliding, and is given By Equation (B.3):

$$\begin{aligned} K_{n,pq} &= \frac{4}{3}E_{eq,pq}\sqrt{\mathrm{R}_{eq,pq}} \\ E_{eq,pq} &= \left(\frac{1-v_p{}^2}{E_p} + \frac{1-v_q{}^2}{E_q}\right)^{-1} \\ \mathrm{R}_{eq,pq} &= \frac{R_p R_q}{R_p + R_q} \end{aligned} \tag{B.3}$$

where $E_{eq,pq}$ is the equivalent Young's Modulus and $R_{er,pq}$ is the equivalent radius of particles p and q. The Poisson's ratio of particles is denoted by v. When the collision happens between a particle and a wall, the equivalent radius takes the value correspondent to radius of the particle. the tangential force is given by (DI RENZO; DI MAIO, 2004):

$$\left|\mathbf{F}_{t,pq}\right| = \min\begin{cases} K_{t,pq}\delta_{t,pq}, & \left|K_{t,pq}\delta_{t,pq}\right| < \left|K_{n,pq}\delta_{n,pq}\right|C_{fs} \\ \dfrac{\left|K_{n,pq}\delta_{n,pq}\right|C_{fs}\delta_{t,pq}}{\left|\delta_{t,pq}\right|}, & \text{otherwise} \end{cases} \tag{B.4}$$

The damping forces acting on both normal and tangential components, indicated by the terms $\mathbf{F}^{d}{}_{n,pq}$ and $\mathbf{F}^{d}{}_{t,pq}$, on Equation (B.1), are given by the following equations (AKHSHIK; BEHZAD; RAJABI, 2015):

$$\mathbf{F}^{d}{}_{n,pq} = -2\sqrt{\frac{5}{6}}\frac{\ln e}{\sqrt{\ln^2 e + \pi^2}}\sqrt{K_{n,pq}m_{eq,pq}}\,\mathbf{v}_{n,pq} \tag{B.5}$$

$$\mathbf{F}^{d}{}_{t,pq} = -2\sqrt{\frac{5}{6}}\frac{\ln e}{\sqrt{\ln^2 e + \pi^2}}\sqrt{K_{t,pq}m_{eq,pq}}\,\mathbf{v}_{t,pq} \tag{B.6}$$

in equations (B.5)and (B.6), $m_{eq,pq}$ is the equivalent mass of the pair of particles colliding. Its expression is given by Equation (B.7) below:

$$m_{eq,pq} = \frac{m_p m_q}{m_p + m_q} \tag{B.7}$$

where m denotes the mass of the particles. When a particle collides with a wall, $m_{eq,pq}$ assumes the value correspondent to mass of the particle. Still in Equation (B.5), $\mathbf{v}_{n,pq}$ is the normal component of the velocity of impact. In Equation (B.6) , $K_{t,pq}$ is the elastic constant on the tangential direction. Its value can be calculated using Equation (B.8):

$$K_{t,pq} = 8G_{eq,pq}\sqrt{\mathrm{R}_{eq,pq}\,\delta_{n,pq}} \tag{B.8}$$

in which G is the equivalent shear modulus of the pair of particles, given by the Equation below:

$$G_{eq,pq} = \left(\frac{1-\nu_p}{G_p} + \frac{1-\nu_q}{G_q} \right)^{-1} \tag{B.9}$$

$$G = \frac{E}{2(1+\nu)}$$

The other equation that must be solved in order to reproduce the behavior of the particle is the equation of the conservation of angular momentum, given by Equation (5). It is rewritten here for commodity:

$$I_p \frac{d\boldsymbol{\omega}_p}{dt} = \mathbf{T}_D + \left(\mathbf{T}^p{}_{t,q} + \mathbf{T}^p{}_{r,q} \right) \tag{B.10}$$

As mentioned in the MATHEMATICAL FORMULATION section, the last two terms in Equation (B.10), both calculated using the Discrete Element Method, are now introduced. $\mathbf{T}^{\mathrm{p}}{}_{\mathrm{t,q}}$ and $\mathbf{T}^{\mathrm{p}}{}_{\mathrm{n,q}}$ represent, respectively, the tangential and normal components of the torque generated by collisions of the particles. Their expressions are given by equations (B.11) and (B.12) (KUANG; YU; ZOU, 2009):

$$\mathbf{T}^p{}_{t,q} = \mathbf{r}_{pq} \times \left(\mathbf{F}_{t,pq} + \mathbf{F}^d{}_{t,pq} \right) \tag{B.11}$$

$$\mathbf{T}^p{}_{\mathrm{r},q} = -R_{fc} \left| \mathbf{r}_{pq} \right| \left| \mathbf{F}_{n,pq} \right| \frac{\boldsymbol{\omega}_{pq}}{\left| \boldsymbol{\omega}_{pq} \right|} \tag{B.12}$$

where $\mathbf{r}_{pq}$ is the vector pointing from the center of mass of particle p to particle's q center of mass.